Sulfide bornite thermoelectric material: natural mineral with ultralow thermal conductivity

Journal:	*Energy & Environmental Science*
Manuscript ID:	EE-COM-07-2014-002428.R2
Article Type:	Communication
Date Submitted by the Author:	22-Sep-2014
Complete List of Authors:	Qiu, Pengfei; shanghai institute of ceramics, zhang, tiansong; Chinese Academy of Sciences, State Key Laboratory of High Performance Ceramics and Superfine Microstructure, Shanghai Institute of Ceramics Qiu, Yuting; Chinese Academy of Sciences, State Key Laboratory of High Performance Ceramics and Superfine Microstructure, Shanghai Institute of Ceramics; Graduate University of Chinese Academy of Sciences, Shi, Xun; shanghai institute of ceramics, chen, lidong; shanghai institute of ceramics, chinese academy of sciences, CAS Key laboratory of Materials for Energy Conversion

SCHOLARONE™
Manuscripts

Energy & Environmental Science

RSCPublishing

COMMUNICATION

Sulfide bornite thermoelectric material: natural mineral with ultralow thermal conductivity

Cite this: DOI: 10.1039/xoxxoooooox

Pengfei Qiu [ab], Tiansong Zhang[b], Yuting Qiu[b], Xun Shi,*[ab] and Lidong Chen*[ab]

Received ooth January 2012,
Accepted ooth January 2012

DOI: 10.1039/xoxxoooooox

www.rsc.org/

Abstract

We report a new type of thermoelectric material, sulfide bornite (Cu_5FeS_4), as a widespread natural mineral composed of non-toxic and earth-abundant elements. Bornite has ultralow thermal conductivity, adjustable electrical transport properties, and enhanced stability under large electric currents, showing a great potential as a new economical and eco-friendly thermoelectric material.

Since the end of last century, the increased concern on environment and energy crisis has shifted the world view on renewable energy sources. One of the most exciting clean energy conversion techniques is using thermoelectric (TE) modules or devices to directly convert energy between heat and electricity without using any moving parts or releasing greenhouse gases.[1,2] Although such kind of technology has been already extensively adopted to power the deep space satellite for long-life missions since 1960s, [3] its development in civil applications, such as solid-state refrigeration and waste heat harvesting generator, is limited because most of the current state-of-the-art TE materials consist of toxic, expensive, or scarce elements (*e.g.* Pb, Te, Ge, Yb, Co).[4-7] The TE technology used for civil applications requires the materials possessing not only high TE performance, but also the ability of economical and environment-friendly large-scale mass production. This pushes the search of novel high performance TE materials with eco-friendly and earth-abundant elements among one of the hottest topics in TE society. [8,9] Towards this goal, silicides and sulfides are two most interesting candidates because of the non-toxic and earth-abundant features of silicon and sulfur. A common view is that sulfides usually possess low zT values on account of sulfur's light atomic weight for large thermal conductivity and strong ionic character for low carrier mobility.[10-12] However, recent two copper-sulfides, $Cu_{12}Sb_4S_{13}$ and $Cu_{2-x}S$, have been reported to show high zTs up to 1.0 and 1.7,[13,14,15] respectively, comparable with the state-of-the-art TE materials. Especially, these two sulfides, named as respective tetrahedrite and chalcocite, are natural minerals which are among the most widespread ores on earth.[16,17] This makes these sulfides more appealing for low-cost and large-scale mass production.

Following this direction, we turn to work on other sulfide materials, in particularly for those natural minerals which have been well-known for many years. Bornite is another widespread copper-sulfide mineral occurring in a variety of ore deposits formed under a wide range of geological conditions.[18] Because Fe donates three electrons and Cu donates one electron, Cu_5FeS_4 should be a semiconductor.[19] It has three temperature-dependent phases, termed high cubic phase, intermediate cubic phase, and low orthorhombic phase.[20] The high cubic phase, existing at temperature above 543 K, has antifluorite-type structure, in which five Cu atoms, one Fe atom, and two vacancies (□) randomly occupy the center of eight sulfur tetrahedrons.[20] In this peculiar crystal structure, the ordered and stiff sulfur framework might supply good electrical transport, while the completely disordered cation distribution can greatly interrupt the thermal transport and lead to low thermal conductivity. In fact, in some degree, this high cubic phase of bornite can be regarded as the Fe and vacancy doped high cubic chalcocite phase (α-Cu_2S), and then the formula can be written as $Cu_5Fe\square_2S_4$. However, until today, the TE transports of bornite have not been reported yet and many of the physical properties are still absent.

In this work, we report the TE transport properties of bornite. Narrow band-gap semiconducting behavior and abnormal ultralow thermal conductivity have been observed in this natural mineral. In addition, by forming the solid-solution with Cu_2S, the electrical transports as well as the TE performance of bornite are easily tuned to achieve a maximum zT of 1.2 at 900 K. More unexpectly and interestingly, we show that bornite is much stable as compared with Cu_2S even under large electric currents.

The crystal structures along the b-axes for the three bornite phases are shown in Fig. 1. At temperature below around 543 K, the high cubic phase (space group $Fm3m$, a = 5.49 Å) transforms to the intermediate cubic phase (space group $Fm3m$, a = 10.950 Å) because of the established Cu/Fe long-rage ordering and vacancy clustering.[21] The structure of this intermediate cubic phase can be regarded as a doubling of the high cubic phase cell along the three crystallographic axes. There are two alternating sub-cells along b-axes, named as M_1 and M_2. The Fe-contained M_1 sub-lattice consists of a random distribution of 8 Cu/Fe atoms, while the Fe-free M_2 sub-lattice consists of 4 Cu atoms and 4 vacancies. Below 473 K, bornite exists in the form of the low orthorhombic phase (space group $Pbca$, $a = c$ = 10.950 Å, b = 21.862 Å), in which the vacancies in each of

This journal is © The Royal Society of Chemistry 2012

the M_2 sub-lattice forming an ordered tetrahedral arrangement as that in the zinc-blend structure.[22] For the two next M_2 sub-lattices along *b*-axis, the orientation of this vacancy tetrahedron alternates which results in a double repeat of the sub-cell of the intermediate cubic phase along *b*-axis. Meanwhile, the Cu/Fe atoms distribution in M_1 sub-cell and the crystal structure characters along *a*- and *c*-axis in the intermediate cubic phase are well maintained.

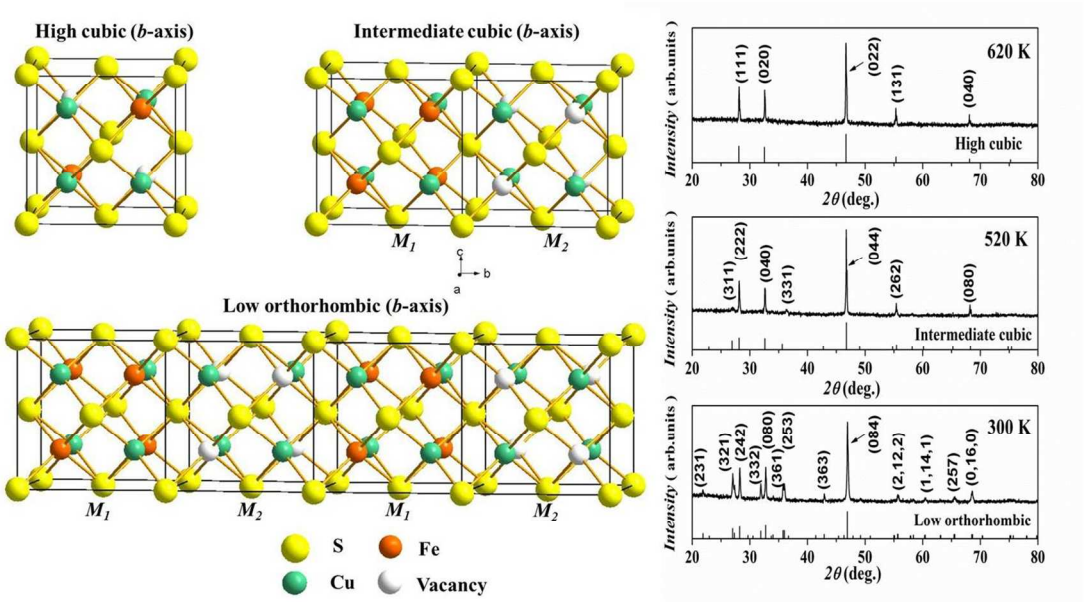

Figure 1. Crystal structures along the b-axes for the high cubic phase, intermediate cubic phase, and low orthorhombic phase of bornite. The XRD diffraction patterns of bornite collected at 300 K, 520 K, and 620 K are shown in the right picture.

Since all the sub-cells in the three bornite phases possess similar crystal structure and lattice parameters, the intermediate cubic phase and low orthorhombic phase can be regarded as the superstructures of the high cubic phase.[20] At elevated temperature, these superstructures vanish because the symmetry is enhanced arising from the re-distribution of Cu/Fe/vacancy. This can be confirmed by the X-ray measurements carried out at specified temperatures, 620 K, 520 K, and 300 K, which are corresponding to the high cubic phase, intermediate cubic phase, and low orthorhombic phase, respectively (see Fig. S1, ESI). As shown in Fig. 1, there are dozens of diffraction peaks in the XRD pattern collected at 300 K but many of them disappear at elevated temperature and only 5 diffraction peaks remain at 620 K. The change of the crystal face index of the left 5 diffraction peaks can well reflect the crystal structure evolution, especially the enhanced symmetry of bornite. For instance, the crystal face index (242) at 300 K first changes to (222) at 520 K because of the destroyed short-range ordering of the vacancies in *b*-axes, and then changes to (111) at 620 K because of the completely disappearance of the Cu/Fe/vacancy long-range ordering in all three axes.

Due to the peculiar crystal structure, bornite is expected to possess interesting electrical and thermal transport properties. Although bornite is stable from ambinent temperatures to in excess of 1373 K,[23] we observed sulfur sublimission on the sample surface above 700 K during the TE property measurements. Thus, here we only present the TE properties below 700 K. The Seebeck coefficient (S) and electrical conductivity (σ) are shown in Fig. 2(a) and (b), respectively. The stoichiometric bornite Cu_5FeS_4 exhibits n-type conducting behavior at low temperature, but it changes to p-type conducting above about 450 K. This transition indicates the dominated electron transport mechanism in Cu_5FeS_4 changes from weak extrinsic conduction to intrinsic conduction, in which the number of carriers thermally excited across the band gap overwhelms the number of carriers induced by ionized impurities. The Seebeck coefficient of Cu_5FeS_4 is very large, but the σ is quite low, only around 5.0 Sm^{-1} at 300 K, as a result of the very low carrier concentration (1.7×10^{16} cm^{-3} at 300 K). Since the σ shows semiconducting behavior throughout the whole temperature range, the thermal activation energy (E_a) of bornite can be calculated based on the empirical relation $\sigma \sim \exp(-E_a/k_BT)$, where k_B is the Boltzmann constant. As shown in Fig. S2 (ESI), the calculated E_a values is 0.16 eV and 0.27 eV for the low orthorhombic phase and high cubic phase of bornite, respectively, typical numbers in the range of narrow band gap semiconductors. These small E_a values suggest that the electrical transport properties in bornite can be easily tuned, as confirmed by the dramatically enhanced σ values for the slightly off-stoichiometric samples with richer Cu and poorer Fe ($Cu_{5.02}Fe_{0.98}S_4$ and $Cu_{5.04}Fe_{0.96}S_4$). Because the valence state of Fe (+3) in bornite is higher than that of Cu (+1),[19] the off-stoichiometry in $Cu_{5.02}Fe_{0.98}S_4$ and $Cu_{5.04}Fe_{0.96}S_4$ can create more hole carriers (*e.g.* 3.9×10^{19} cm^{-3} for $Cu_{5.02}Fe_{0.98}S_4$ at 300 K) and thereby resulting in about 2-3 orders of magnitude higher σ values than that of the Cu_5FeS_4. Meanwhile, the off-stoichiometric bornite samples still maintain large S values, and the maximum S exceeds 200 μVK^{-1}. Combining the tuned σ and S, the maximum power factor ($PF = S^2\sigma$) around 3.5 $\mu Wcm^{-1}K^{-2}$ at 700 K (see Fig. S3, ESI) is achieved in sample $Cu_{5.04}Fe_{0.96}S_4$.

As shown in Fig. 2(c), all three bornite samples exhibit abnormally ultralow thermal conductivity (κ). Each κ curve has a sharp peak around 10 K and a crossover around 500 K. The former one suggests that bornite is a normal crystalline compound,[24] which is consistent with the ordered crystal structure of the low orthorhombic phase. The latter one is related to the phase transition in bornite since the physical properties are different between the high cubic and intermediate cubic phases. Generally, κ consists of the carrier part κ_c and the lattice part κ_L.[24] Here, κ_c could be ignored and the κ_L is equal to the total κ because of the small electrical conductivity. Thus, κ_L in the stoichiometric ratio compound Cu_5FeS_4 shows a maximum value of 1.7 $Wm^{-1}K^{-1}$ at 10 K and subsequently

This journal is © The Royal Society of Chemistry 2012

an ultralow value around 0.2-0.5 $Wm^{-1}K^{-1}$ from 100 K to 700 K. In the off-stoichiometric bornite samples, $Cu_{5.02}Fe_{0.98}S_4$ and $Cu_{5.04}Fe_{0.96}S_4$, the κ_L peak value appearing around 10 K is greatly decreased from 1.7 $Wm^{-1}K^{-1}$ to 0.68 $Wm^{-1}K^{-1}$ as a result of the extra mass or strain fluctuations between Cu and Fe in bornite,[25] while the ultralow κ_L character is still maintained at temperature above 100 K. For comparison, the κ_L values of the state-of-the-art TE materials (Bi_2Te_3[4], PbTe[5], and SiGe[6]) and some other sulfides (TiS_2[10], PbS[11], $CuFeS_2$[12], $Cu_{12}Sb_4S_{13}$[13], and Cu_2S[15]) are ploted in Fig. S4 (ESI) together with those of bornite. Obviously, bornite has much lower κ_L than most of these TE materials reported before.

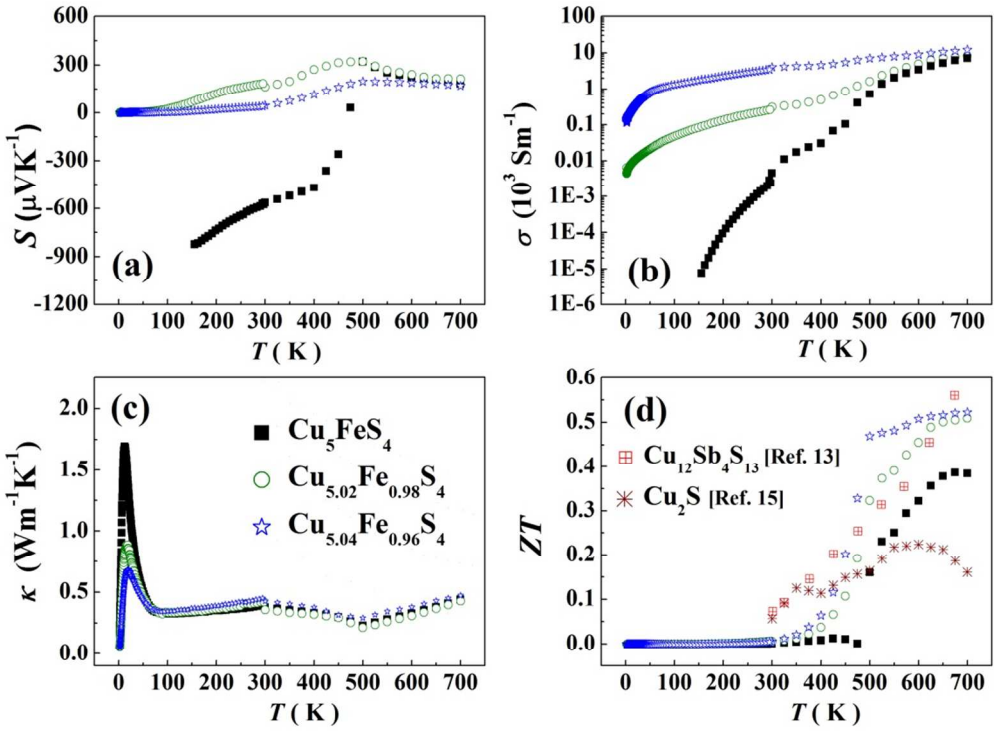

Figure 2. Temperature dependence of (a) Seebeck coefficient, (b) electrical conductivity, (c) thermal conductivity, and (d) the dimensionless figure of merit of bornite samples. The Seebeck coefficient and electrical conductivity for Cu_5FeS_4 below 150 K are not shown because the data are out of the measurement range of PPMS. The *zT* data for the stoichiometric $Cu_{12}Sb_4S_{13}$ and Cu_2S are also included in Fig. 2(d) for comparison.[13,15]

The ultralow κ_L in bornite is very interesting since usually sulfides (*e.g.* TiS_2, PbS, and $CuFeS_2$) have large thermal conductivity (see Fig. S4, ESI) because of the light atomic mass of sulfur and relatively strong chemical bonds between sulfur and the metallic-ions.[10-12] On one hand, the completely disordered distribution of Cu, Fe, and vancancy in the high cubic phase of bornite might greatly interrupt the normal thermal phonon transport and responsible for the ultralow κ_L. On the other hand, due to the same crystal structure and similar composition of bornite with α-Cu_2S, the liquid-like Cu-ions, which cause the abnormal thermal transport behavior in α-Cu_2S,[15] should also exist in bornite and partially contribute to the ultralow κ_L.[26,27] Interestingly, such ultralow κ_L is observed not only at high temperatures, but also at low temperatures in which bornite shows typical crystalline-like thermal transport behavior. We calculate the phonon mean free path (l) in the low orthorhombic phase of bornite according to the relationship $\kappa_L = C_v v_{avg} l/3$ under the hypothesis that the heat capacity at constant volume (C_v) is equal to the theoritical heat capacity at constant pressure (C_p), about 0.474 $JK^{-1}g^{-1}$ for bornite at 300 K, estimated using the Neumann-Kopp law.[28] The l value is 2.3 Å at 300 K, very close to the shortest atomic distance in bornite, about 2.369 Å between Cu/Fe atom and sulfur atom.[22] This suggests that the κ_L has been already close to the minimum thermal conductivity in this natural mineral,[7,29-31] consisting of only light elements Cu, Fe, and S. Such abnormal low κ_L in the low orthorhombic phase of bornite could be partially explained by its inherent large and complex crystal structure, in which 64 S atoms, 80 Cu atoms, 16 Fe atoms, and 32 vacancies form an ultra-large unit cell. This large unit cell volume (> 2600 $Å^3$) can increase the complexity of the phonon density of states and effectively reduces the contribution of acoustic modes to the total thermal transports.[32] In addition, Ding *et al.*reported that there are two or more kinds of superstructure domains coexisting in the low orthorhombic phase of bornite.[33] These nanoscale domains can also introduce abundant additional phonon scattering sources and lead to the low κ_L.

In order to further understand the ultralow κ_L value observed in the low orthorhombic phase of bornite, the low temperature C_p of Cu_5FeS_4 was measured. As shown in Fig. 3, the measured C_p value at 300 K is 0.478 $JK^{-1}g^{-1}$, close to the theoretical value (0.474 $JK^{-1}g^{-1}$). The insert in Fig. 3 displays the heat capacity below 10 K in the C_p/T vs T^2 representation. The dashed line is the fitted curve based on the Debye mode, in which the total C_p only includes the carrier contribution φT and phonon contribution ($\beta T^3 + \alpha T^5$).[34] The fitted parameters are 0.72 $mJmol^{-1}K^{-2}$ for φ, 1.22 $mJmol^{-1}K^{-4}$ for β, and 0.026 $mJmol^{-1}K^{-6}$ for α. The small φ value as compared with other TE materials (*e.g.* $YbFe_4Sb_{12}$, φ = 141.2 $mJmol^{-1}K^{-2}$) indicates the electron density of states near the Fermi level is quite weak at low temperature.[35] This is consistent with the observed very low σ in bornite at low temperatures. The unneglectable fitted α value suggests that there is a huge contribution to C_p from the T^5 term,

which is usually related with the presence of complex phonon density of states.[36] Based on the fitted value β, the Debye temperature (Θ_D = 251 K) can be obtained by the equation $\Theta_D=(12\pi^4pR/5\beta)^{1/3}$, where p is the atom number per chemical formula, R is the molar gas constant.[34] Then, the related physical parameters, such as the average sound velocity (v_{avg} = 2152 ms^{-1}) and the Grűneisen parameter (γ = 3.45) are calculated using the equations shown in the Electronic Supplementary Information (ESI) and they are listed in Table I. It is known that the Grűneisen parameter can well reflect the strength of the lattice anharmonicity in a solid and generally large γ corresponds to low κ_L.[37] Interestingly, the calculated γ value in bornite is extremely high and its value is comparable to those typical TE materials such as SnSe (γ = 4.1 in a axes) [37] and $AgSbSe_2$ (γ = 3.5)[38], in which ultralow κ_L values have been also reported. Such abnormal high γ indicates that there might be some soft modes in bornite due to the existence of the vacancies in the crystal structure and possible strong anharmonicity in bonding. These soft modes contribute to the complex phonon density of states in bornite, as confirmed by the huge T^5 term contribution to C_p, and thereby drastically affecting the normal phonon transport and leading to the ultralow κ_L.

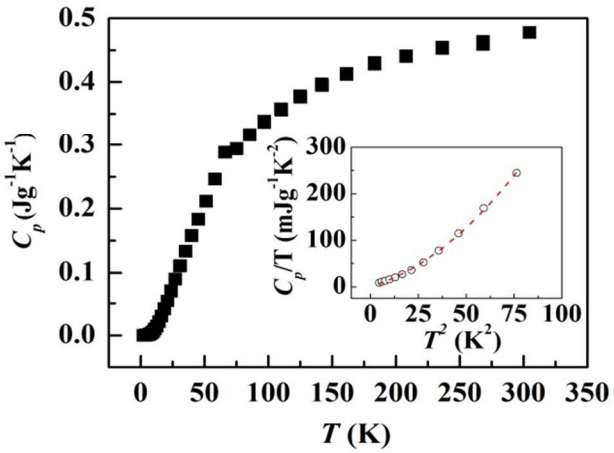

Figure 3. Temperature dependence of heat capacity (C_p) for Cu_5FeS_4 below room temperature. The insert shows the heat capacity below 10 K in the C_p/T vs T^2 representation. The dashed line is the fitted curve for $C_p/T = \varphi + \beta T^2 + \alpha T^4$.

Table I. Thermal Activation energy (E_a), electrical conductivity (σ), Seebeck coefficient (S), Hall carrier concentration (p_H), lattice thermal conductivity (κ_L), heat capacity (C_p), phonon mean free path (l), Debye temperature (Θ_D), averaged speed of sound (v_{avg}), and Grűneisen parameter (γ) of Cu_5FeS_4 at 300 K.

E_a (eV)	S (μVK^{-1})	σ (Sm^{-1})	p_H (10^{16}cm^{-3})	κ_L (Wm^{-1}K^{-1})	C_p (Jg^{-1}K^{-1})	l (Å)	Θ_D (K)	v_{avg} (ms^{-1})	γ
0.16	-565.5	5.0	1.7	0.38	0.478	2.3	251	2152	3.45

Based on the measured S, σ, and κ, the dimensionless figure of merit ($zT= S^2\sigma T/\kappa$), which directly determines the energy conversion efficiency of a TE material, is calculated and shown in Fig. 2(d). The ultralow κ_L ensures the zT reaches a maximum value around 0.38 for the stoichiometric Cu_5FeS_4, and 0.52 for the off-stoichiometric sample $Cu_{5.04}Fe_{0.96}S_4$. These zT values are comparable to the other two TE natural minerals Cu_2S and $Cu_{12}Sb_4S_{13}$, as shown in Fig. 2(d).[13,15]

Similar with $Cu_{12}Sb_4S_{13}$ reported by Lu *et al.*,[13] bornite also shows a quite broad space to tune TE properties. Here we show the the first step to optimize the TE properties by forming solid-solutions with Cu_2S because Cu_2S has the same crystal structure as bornite at high tempeartures. The formula of these solid-solutions can be written as $m$$Cu_8S_4$-(1-$m$)$Cu_5Fe\square_2S_4$ (m = 0.2, 0.5, 0.8 in this study). All the solid-solutions consist at least two phases at room temperature but they gradually transfer to pure cubic phase at high temperatures (see Fig. S5, ESI). Surprisingly, sulfur sublimission is greatly suppressed in the solution samples even at the temperature as high as 900 K. Thus the TE properties of the solution samples up to 900 K are presented in Fig. 4. The σ for all solid-solutions firstly increase when increasing temperature, showing typical semiconducting transport behavior, and then reach a maximum value at elevated temperatures. Because the two ends Cu_2S and Cu_5FeS_4 are ideally semiconductors, the solution samples are expected semiconductors too, which is confirmed by the transport data shown in Fig. 4. Significantly enhanced σ values are observed in the solid-solutions, which is believed to be related with the presence of Cu deficiency in these solid-solutions (see Fig.S5, ESI).[15,39] Because of the enhanced σ and almost undegraded S, the *PFs* of the solid-solutions are greatly increased as compared with that of Cu_5FeS_4 and the maximum value reaches 7.1 μWcm^{-1}K^{-2} at 900 K for 0.8Cu_8S_4-0.2$Cu_5Fe\square_2S_4$ (see Fig. S6, ESI). Meanwhile, the κ of these solid-solutions maintain the relative low values in the whole measured temperature. Combining the measured σ, S, and κ, the zTs for these solid-solutions are calculated. The maximum zT around 1.2 at 900 K is achieved in 0.8Cu_8S_4-0.2$Cu_5Fe\square_2S_4$, comparable with the well-optimized doped-$Cu_{12}Sb_4S_{13}$ materials reported by Lu *et al.*.[4-7,13] Especially, this zT enhancement occurs not only at high temperature but also throughout the whole measured temperature range. For instance, the zT for 0.8Cu_8S_4-0.2$Cu_5Fe\square_2S_4$ at 700 K is 0.85, about two times higher than that of bornite.

This journal is © The Royal Society of Chemistry 2012

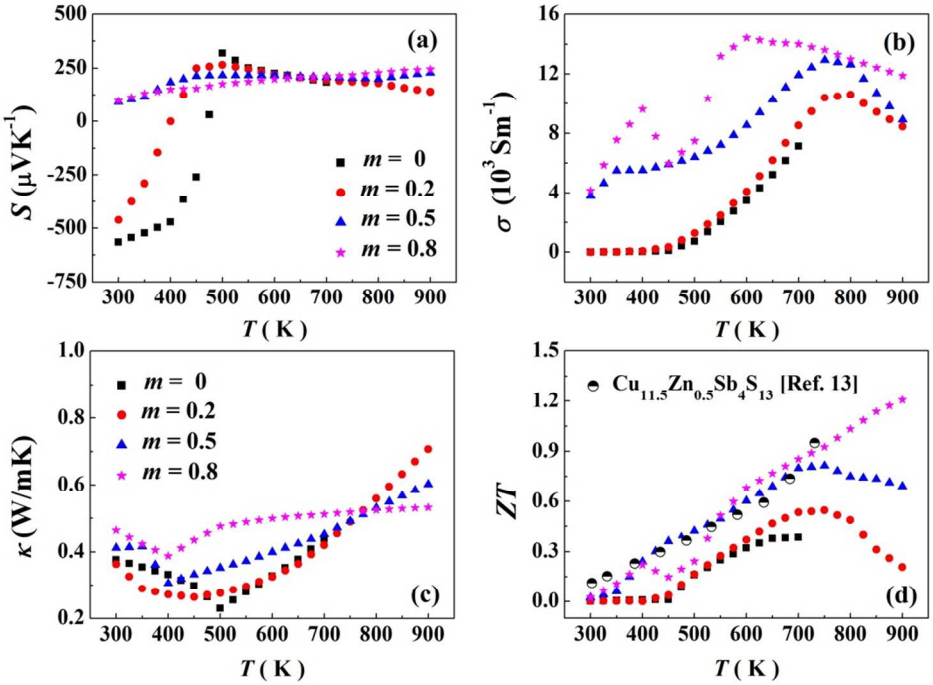

Figure 4. Temperature dependence of (a) Seebeck coefficient, (b) electrical conductivity, (c) thermal conductivity, and (d) the dimensionless figure of merit of $m$$Cu_8S_4$-(1-$m$)$Cu_5Fe\square_2S_4$ (m = 0.2, 0.5, 0.8) solid-solutions. The zT data for the optimized $Cu_{12}Sb_4S_{13}$ sample reported by Lu *et al*. are also included in Fig. 4(d) for comparison.[13]

In addition the abnormal TE properties, bornite Cu_5FeS_4 also displays unexpected and interestingly high stability under large electric current because of the pinning effect of Fe atoms on the Cu-site which can greatly suppress the migration of copper ions. One of key challenges for Cu-based TE materials and device is fast Cu-ion migration under large currents or temperature gradient, which can quickly degrade the TE performance or even destroy the initial material's crystal structure.[40] This issue has been reported by Miyatani *et al*. in Cu_2S system about 60 years ago.[41] Recently, Dennler *et al.* further demonstrated the severe Cu-ion migration in Cu_2S at room temperature under 12 Acm^{-2} current density, which is believed the maximum standard value in TE generator devices.[42] In the present study, we carried out the intermediate temperature test (at 573 K) for sample Cu_2S and bornite under the current density of 12 Acm^{-2} to characterize the degree of Cu-ion migration. Since the hole concentration and electrical resistance in these Cu-based compounds are sensitive to the amount of Cu deficiencies,[15] the Cu-ion migration under large current can create more Cu deficiencies in the matrix and significantly reduce the electrical resistance. Therefore, the change of relative electrical resistance (R/R_0) well reflects the migration degree of Cu ions in these Cu-based materials, where R_0 is the initial electrical resistance and R is the electrical resistance under large currents. As shown in Fig. 5, R/R_0 for Cu_2S quickly decreases to around 45% after only 5 seconds, and to about 10% after 2000 seconds. The R/R_0 variation between 60 and 2000 seconds might be related to the crystal structrue transition from hexagonal Cu_2S to cubic $Cu_{2-x}S$.[43] However, this huge drop in electrcial resistance is greatly suppressed in bornite although its crystal structure is similar to Cu_2S at high temperatures. The electrical resistance in bornite is reduced to 95% after 1000 seconds and to 90% after about 60000 seconds, as shown in Fig. 5. No abrupt R/R_0 variation is observed in bornite even after 60000 seconds tested at high temperaures, indicating a much stable crystal structure. By comparing bornite with Cu_2S, we believe the immobile Fe atoms play the pinning effect to suppress the Cu-ion migration. In particular, Fe atoms are randomly located at the same crystallographically sites as the mobile Cu ions, and thus the migration channels of Cu ions can be significantly blocked or interrupted. Although we just provide a very simple test in the present work, our data suggest that the liquid-like ions in superionic TE materials can be suppressed or just localized at a small scope to improve material's stability for real applications.

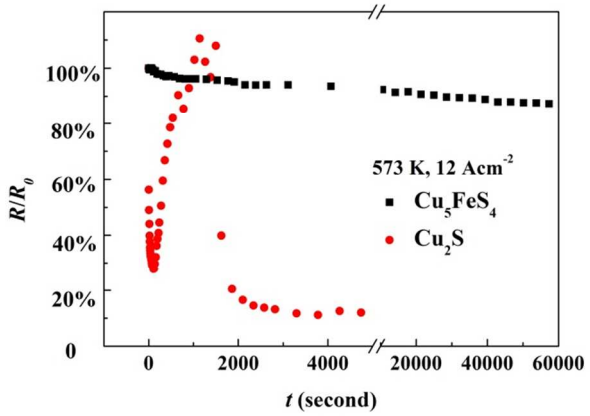

Figure 5. Relative electrical resistance of Cu_2S and Cu_5FeS_4 as a function of current stress duration at 573 K under a current density of 12 Acm^{-2}.

In summary, we report the TE properties of sulfide bornite, Cu_5FeS_4, as a widespread natural mineral with ultralow thermal conductivity. This material is a narrow band-gap semiconductor with the order-disorder distributions of Cu/Fe/vacancy in the sulfur framework. Ultralow κ and a quite broad space for TE properties optimization have been demonstrated in this system. Especially, we show that the migration of Cu ions in bornite is hugely suppressed as

compared with that in Cu_2S due to the pinning effect of immobile Fe atoms.

Experiment section

High purity elements Cu (shot, 99.999%, Alfa aesar), Fe (piece, 99.99%, Alfa aesar), and S (piece, 99.9999%, Alfa aesar) were weighed out in the atomic ratio of $Cu_{5+x}Fe_{1-x}S_4$ (x = 0, 0.02, 0.04), and then sealed in the evacuated quartz ampoules which were coated with carbon. The sealed ampoules were heated slowly up to 1273 K at a speed of 2 $Kmin^{-1}$ and then remained at this temperature for 20 hours before quenching into a water bath. Next, the ingots were annealed at 873 K for 5 days. To form dense pellets, the obtained ingots were manually ground into fine powders (< 100 μm) and then sintered by Spark Plasma Sintering (SPS) at 773 K for 5 minutes. High-density (> 98% of the theoretical density) were obtained for all samples.

X-ray diffraction analysis (D8 ADVANCE, Bruker Co. Ltd) was used to examine the purity and chemical composition of Cu_5FeS_4 at specified temperatures. Differential scanning calorimetry (DSC) measurement was carried out from 300 K to 700 K to detect the phase transition in Cu_5FeS_4 using DSC 200 F3 (Netzsch Co. Ltd). The relative length change ($\Delta L/L_0$) of Cu_5FeS_4 in the heating process was measured using the DIL 402 C (Netzsch Co. Ltd). Below room temperature, electrical conductivity, Seebeck coefficient, heat capacity, and thermal conductivity were measured in a Physical Property Measurement System (PPMS, Quantum Design) from 2 K to 300 K under vacuum. Above room temperature, electrical conductivity and Seebeck coefficient were measured using the ZEM-3 (ULVAC Co. Ltd.) apparatus under Helium atmosphere. Thermal conductivity above room temperature was calculated by multiplying the measured values of thermal diffusivity, heat capacity, and density. The thermal diffusivity was measured in argon atmosphere using laser flash method (LFA 427, Netzsch Co. Ltd). The heat capacity (C_p = 0.474 $JK^{-1}g^{-1}$) is estimated using the Neumann-Kopp law. The density of the samples was measured using Archimedes method. Hall coefficients (R_H) at 300 K were measured in PPMS by sweeping the magnetic field up to 3 T in both positive and negative directions. The samples with the size of about 2×2×4 mm^3 were put between two copper blocks and then loaded in a furnance. After the furnance temperature was stabilized at 573 K for 10 hours, the samples were stressed under a current with a density of 12 Acm^{-2} and hold this state for a long time. The electrical resistance was measured at slected current stress durations.

Acknowledgments

This work is in supported by National Basic Research Program of China (973-program) under Project No. 2013CB632501, and National Natural Science Foundation of China (NSFC) under the No. 5112064 and 51222209.

Notes and references

[a] State Key Laboratory of High Performance Ceramics and Superfine Microstructure, Shanghai Institute of Ceramics, Chinese Academy of Sciences, 1295 Dingxi Road, Shanghai 200050, China.

[b] CAS Key Laboratory of Materials for Energy Conversion, Shanghai Institute of Ceramics, Chinese Academy of Sciences, Shanghai, 200050, China.

† Electronic Supplementary Information (ESI) available: some physical parameters calculation details; DSC scan profile (Fig.S1) and thermal activation energy (Fig.S2) for Cu_5FeS_4; Power factor for bornite samples (Fig.S3); Temperature dependence of lattice thermal conductivities for bornite and some reported TE materials (Fig.S4); XRD diffraction patterns of $0.5Cu_8S_4$-$0.5Cu_5Fe\square_2S_4$ solid solution (Fig.S5); Power factor for $m Cu_8S_4$-$(1-m)Cu_5Fe\square_2S_4$ solid solutions.

See DOI: 10.1039/c000000x/

1 A. F. Ioffe, Semiconductor Thermoelements and Thermoelectric Cooling, London, 1957.
2 L. E. Bell, Science 2008, **321**,1457.
3 G. A. Slack, CRC handbook of Thermoelectrics, Boca Raton: CRC press.
4 B. Poudel, Q. Hao, Y. Ma, Y. Lan, A. Minnich, B. Yu, X. Yan, D. Wang, A. Muto, D. Vashaee, X. Chen, J. Liu, M. Dresselhaus, G. Chen, and Z. Ren, Science 2008, **320**, 634.
5 Y. Pei, X. Shi, A. Lalonde, H. Wang, L. Chen, and G. J. Snyder, Nature 2011, **473**, 66.
6 G. Joshi, H. Lee, Y. Lan, X. Wang, G. Zhu, D. Wang, R. Gould, D.C. Cuff, M.Y. Tang, M.S. Dresselhaus, G. Chen, and Z. Ren, Nano Letter, 2008, **8**, 4670.
7 X. Shi, J.Yang, J. R. Salvador, M. Chi, J. Y. Cho, H. Wang, S. Bai, J. Yang, W. Zhang, and L. Chen, J. Am. Chem. Soc. 2012, **133**, 7837.
8 M. He, J. Ge, Z. Lin, X. Feng, X. Wang, H. Lu, Y. Yang, and F. Qiu, Energy Environ. Sci., 2012, **5**, 8351.
9 M. He, F. Qiu, and Z. Lin, Energy Environ. Sci., 2013, **6**, 1352.
10 M. Beaumale, T. Barbier, Y. Bréard, S. Hébert, Y. Kinemuchi, and E. Guilmeau, J. Appl. Phys. 2014, **115**, 043704.
11 H. Wang, E. Schechtel, Y. Pei, and G. J. Snyder, Adv. Energy Mater. 2013, **3**, 488.
12 J. Li, Q. Tan, and J-F. Li, J. Alloys. Compd. 2013, **551**, 143.
13 X. Lu, D. T. Morelli, Y. Xia, F. Zhou, V. Ozolins, H. Chi, X. Zhou, and C. Uher, Adv. Energy Mater. 2013, **3**, 342.
14 X. Lu and D. T. Morelli, Phys. Chem. Chem. Phys. 2013, **15**, 5762.
15 Y. He, T. Day, T. Zhang, H. Liu, X. Shi, L. Chen, and G. J. Snyder, Adv. Mater. 2014, **26**, 3974.
16 A. Pfitzner, M. Evain, and V. Petricek, Acta Crystallographica 1997, **B53**, 337.
17 H. T. Evans, Nature Phys. Sci. 1971, **232**, 69.
18 B. A. Grguric and A. Putnis, Canada. Miner. 1998, **36**, 215.
19 G. van der Laan, R. A. D. Pattrick, J. M. Charnock, and B. A. Grguric, Phys. Rev. B 2002, **66**, 045104.
20 B. A. Grguric, A. Putnis, and R. J. Harrison, Ameri. Mineralogist 1998, **83**, 1231.
21 Y. Kanazawa, K. Koto, and N. Morimoto, Canada. Miner. 1978, **16**, 397.
22 K. Koto, N. Morimoto, Acta Crystallographica 1975, **B31**, 2268.
23 R. A. Robie, R. R. Seal, B. S. Hemingway, Canada. Miner. 1994, **32**, 945.
24 G. A. Slack, Solid State Phys. 1979, **34**,1.
25 J. Yang, G. P. Meisner, and L. D. Chen, Appl. Phys. Lett. 2004, **85** 1140.
26 H. L. Liu, X. Shi, F. F. Xu, L. L. Zhang, W. Q. Zhang, L. D. Chen, Q. Li, C. Uher, D. Tristan, and G. J. Snyder, Nat. Mater. 2012, **11**,422.
27 H. L. Liu, X. Yuan, P. Lu, X. Shi, F. F. Xu, Y. He, Y. S. Tang, S. Q. Bai, W. Q. Zhang, L. D. Chen, Y. Lin, L. Shi, X. Y. Gao, X. M. Zhang, H. Chi, C. Uher, Adv. Mater. 2013, **25**, 6607.
28 C. N. Bhandari and D. M. Rowe, Thermal Conduction in Semiconductors, London, 1988.
29 D. T. Morelli, V. Jovovic, and J. P. Heremans, Phys. Rev. Lett. 2008, **101**, 035901.
30 T. Zhou, B. Lenoir, M. Colin, A. Dauscher, R. A. Orab, P. Gougeon , M. Potel, and E. Guilmeau, Appl. Phys. Lett. 2011, **98**, 162106.
31 J. Y. Cho, X. Shi, J. R. Salvador, G. P. Meisner, J. Yang, H. Wang, A. A. Wereszczak, X. Zhou, and C. Uher, Phys. Rev. B 2011, **84**, 085207.
32 E. S. Toberer, A. F. May, and G. J. Snyder, Chem. Mater. 2010, **22**, 624.
33 Y. Ding, D. R. Veblen, and C. T. Prewitt, Ameri. Mineralogist 2005, **90**, 1256.
34 E. S. R. Gopal, Specific Heat at Low Temperatures, London, 1966.

 This journal is © The Royal Society of Chemistry 2012

35 W. Schnelle, A. Leithe-Jasper, H. Rosner, R. Cardoso-Gil, R. Gumeniuk, D. Trots, J. A. Mydosh, and Yu. Grin, Phys. Rev. B 2008, **77**, 094421.
36 Y. Nakajima, T. Nakagawa, T. Tamegai, and H. Harima, Phys. Rev. Lett. 2008, **100**, 157001.
37 L-D Zhao, S-H Lo, Y. Zhang, H. Sun, G. Tan, C. Uher, C. Wolverton, V. P. Dravid, and M. G. Kanatzidis, Nature 2014, **508**, 373.
38 M. D. Nielsen, V. Ozolins, and J. P. Heremans, Energ. Environ. Sci. 2013, **6**, 570.
39 Q. Jiang, H. Yan, J. Khaliq, Y. Shen, K. Simpson, and M. J. Reece, J. Mater. Chem. A 2014, **2**, 9486.
40 D. R. Brown, T. Day, T. Caillat, and G. J. Snyder, J. Elect. Mater. 2013, **42**, 2014.
41 S.–Y. Miyatani, Y. Suzuki, J. Phys. Soc. Jpn. 1953, **8**, 680.
42 G. Dennler, R. Chmielowski, S. Jacob, F. Capet, P. Roussel, S. Zastrow, K. Nielsch, I. Opahle, and G. K. H. Madsen, Adv. Energ. Mater. 2014, 1301581.
43 W. R. Cook, Solid State Chem. 1972, **364**, 703.

Graphical Abstract

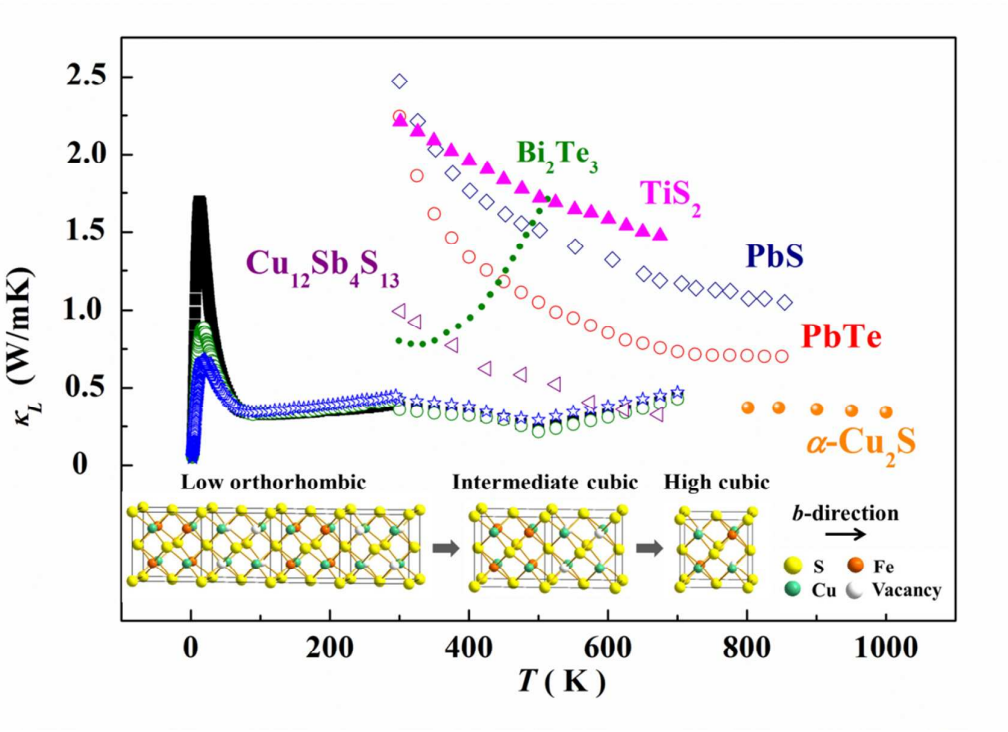

Natural mineral bornite with ultralow thermal conductivity exhibits excellent thermoelectric performance and enhanced stability under large electric currents.